Published in final edited form as:
*Biochemistry*. 2008 June 24; 47(25): 6602–6611. doi:10.1021/bi8004279.

# DIRECT LOADING OF PURIFIED ENDOGENOUS INHIBITOR INTO THE CYTOPLASM OF PATCHED CARDIOMYOCYTES BLOCKS THE ION-CURRENTS AND CALCIUM TRANSPORT THROUGH THE NCX1 PROTEIN

**Liron Boyman**[§], **Reuben Hiller**[§], **W. Jonathan Lederer**[¶], and **Daniel Khananshvili**[§,1]

[§] Department of Physiology and Pharmacology, Sackler School of Medicine, Tel-Aviv University, Ramat-Aviv 69978, Israel

[¶] Medical Biotechnology Center, University of Maryland Biotechnology Institute, Baltimore, Maryland 21201

## Abstract

The $Na^+/Ca^{2+}$ exchanger in mammalian heart muscle (NCX1) is the central transporter protein that regulates $Ca^{2+}$ extrusion from the heart cell. However, the functional biochemistry and physiology of NCX1 has been severely hampered by the absence of any specific high-affinity inhibitor. Here we describe advanced procedures for purifying a candidate inhibitor, previously called endogenous inhibitor factor ($NCX_{IF}$) and demonstrate its direct actions on NCX1 activities in the single cell system. A combination of advanced HILIC (Hydrophilic Interaction Liquid Chromatography) procedures with analytical tests suggests that $NCX_{IF}$ resembles the properties of small (disaccharide size) polar molecule lacking any aromatic rings, conjugated bonds, or primary amino group. The effects of $NCX_{IF}$ on the NCX1-mediated ion-currents ($I_{NCX}$) and cytosolic $Ca^{2+}$-extrusion were detected by a combination of patch-clamp and confocal microscopy under conditions at which the purified $NCX_{IF}$ was directly loaded into the cytoplasm of patched cardiomyocytes. It was demonstrated that cytosolic $NCX_{IF}$ blocks the $Ca^{2+}$-activated NCX1 inward current and the accompanying $Ca^{2+}$-extrusion from the cell with high efficacy. A constant fraction of NCX1 inhibition was observed under conditions at which the cytosolic $[Ca^{2+}]_i$ was varied at fixed doses of $NCX_{IF}$, suggesting that the degree of inhibition is controlled by $NCX_{IF}$ dose and not by cytosolic $Ca^{2+}$ concentrations. $NCX_{IF}$ blocks equally well both the $Ca^{2+}$ extrusion and $Ca^{2+}$ entry modes of NCX1, consistent with thermodynamic principles expected for the functioning of a bidirectional “carrier-type” transport system. We concluded that $NCX_{IF}$ interacts with a putative regulatory domain from the cytosolic side and thus, may play an important regulatory role in controlling $Ca^{2+}$ signaling in the heart. This may represent a new potential tool for developing novel treatments for cardiac $Ca^{2+}$ signaling dysfunction.

Proteins of the NCX gene family contribute to $Ca^{2+}$ regulation in many cell types (1–4), with three genes responsible for expression, namely, NCX1, NCX2, and NCX3 with multiple splice variants (2,5–7). In heart, the electrogenic $Na^+/Ca^{2+}$ exchange (8) is due to the gene product of NCX1.1 and, although the molecular and biophysical properties have been broadly studied (2–7), endogenous regulation is incompletely understood (9–13). Nevertheless, it is clear that changes in NCX1 protein expression accompany the development of diverse diseases such as heart failure and arrhythmia (2–4,9). There is, however, considerable uncertainty regarding the role played by NCX1 in these diseases and,

[1]Address Correspondence to: Daniel Khananshvili, Department of Physiology and Pharmacology, Sackler School of Medicine, Tel-Aviv, University, Ramat-Aviv 69978, Israel; Tel:972-3-640-9961; Fax: 972-3-640-9113; dhanan@post.tau.ac.il.

moreover, to date, there is neither evidence that the NCX1 activity is the *primary* cause of such diseases nor are mutations of NCX1 linked to any specific disease. Nevertheless, NCX1 protein levels may change and certainly contribute to $Ca^{2+}$ transport and signaling dysfunction, although the details remain poorly understood (2–4,9).

The $Na^+/Ca^{2+}$ exchanger turnover rate is clearly affected by the intracellular $Ca^{2+}$, $Na^+$, and $H^+$ ions, which interact with the regulatory cytosolic f-loop of NCX proteins (3,4,10–13). Other cellular factors (ATP, $PIP_2$, and lipids) also can modulate NCX1, but their physiological relevance is still unclear (11,12). No phosphorylation of the cardiac NCX1 protein has been demonstrated either *in vitro* or *in vivo*. Recent breakthroughs in elucidating the 3D structure revealed that the f-loop contains two $Ca^{2+}$-binding domains, CBD1 and CBD2 (14–16), which may modulate the NCX1 activity by sensing the cytosolic $Ca^{2+}$ concentrations. If specific endogenous factors exist, affecting the $Ca^{2+}$ interactions with the cytosolic regulatory domains, they may be quite important.

We isolated (from calf ventricle extracts) and purified a low molecular substance that inhibits NCX1 in sarcolemma vesicles (17,18). Mass-spectroscopic and gel-filtration analyses of active substances revealed a small (350–550 Da) polar molecule that is not retained on the regular RP-HPLC columns (17,18). Chemical tests and spectroscopic analyses showed no content for conjugated bonds, aromatic rings, primary amines, or aldehyde groups, thereby resembling the properties of non-reducing “sugar-like” molecules (17,18). This low-abundance compound inhibits NCX1 activites in the range of $10^{-6}$–$10^{-7}$ M (18), but it has no effect on the $Na^+/K^+$-ATPase or SR $Ca^{2+}$-ATPase activities (19). This compound was termed “the NCX inhibitory factor” or $NCX_{IF}$.

Application of $NCX_{IF}$ to organ bath solutions elevates the contractility of ventricle strips (17,20), meaning that $NCX_{IF}$ could be a physiologically active substance. Importantly, the $\beta_1$-blocker (deraline) does not affect these actions (20), suggesting that $NCX_{IF}$ may act through a mechanism that is independent of the β-adrenergic pathway. Moreover, $NCX_{IF}$ could suppress ouabain-induced arrhythmias, thereby resembling the properties of anti-arrhythmic agents (23). This suppression of arrhythmia may represent the $NCX_{IF}$-induced block of $Ca^{2+}$ activated inward $I_{NCX}$ (triggered during $Ca^{2+}$ overload).

Extracellular perfusion of electrically paced cardiomyocytes with $NCX_{IF}$ resulted in enhanced amplitudes of cell contractions and of $[Ca^{2+}]_i$ transients (22). Although these observations can be rationally explained by primary inhibition of NCX1 in the cell, no evidence existed for this claim. The reason for this lack of information was that no patch-clamp techniques were applied at this time for testing the $NCX_{IF}$ effects in a single-cell system. Therefore, in the present work the effects of $NCX_{IF}$ on $I_{NCX}$ currents and $Ca^{2+}$-extrusion were tested under conditions at which $NCX_{IF}$ was directly loaded into the cytoplasm of patched cardiomyocytes. Here, the cytosolic $[Ca^{2+}]_i$ was transiently elevated (by exposing cardionyocytes to caffeine for short periods), whereas the $I_{NCX}$ and $[Ca^{2+}]_i$ signals were subsequently recorded with patch-clamp and confocal microscopy.

If NCX1 is affected by $NCX_{IF}$, it is also important to know where on the protein $NCX_{IF}$ acts. Kinetic studies with sarcolemma vesicles suggested that $NCX_{IF}$ acts as a non-competitive inhibitor with respect to extra-vesicular (cytosolic) $Ca^{2+}$ (21). This was taken to mean that $NCX_{IF}$ interacts with a regulatory (but not transport) site on NCX1 protein and may thereby alter the rate-limiting step of the ion-transport cycle. In intact cells, the time of action of extracellularly applied $NCX_{IF}$ on contractility and $[Ca^{2+}]_i$ transients was quite slow (5–15 min), suggesting that $NCX_{IF}$ must enter the cell to act (20,22). To test the sidedness of the action of $NCX_{IF}$, we directly loaded purified $NCX_{IF}$ into the cytoplasm through the patch clamp electrode and examined the action of $NCX_{IF}$ on $I_{NCX}$ and $Ca^{2+}$-

extrusion. We provide strong evidence that $NCX_{IF}$ blocks NCX1 from the inside of the cell with great efficacy, meaning that $NCX_{IF}$ may be an endogenous regulator of $Ca^{2+}$ transport through the regulation of NCX1 in intact cells.

## Materials and Methods

### Materials and reagents

Protease inhibitors (PMSF, pepstatin, leupeptin, and aprotenin), Deoxyribonuclease I (type DN-25), fluorescamine, Dowex-50W 1×8, Dowex-AG 1×4, and laminin were obtained from Sigma (St. Louis, MO). Sephadex G-10 (fine) was from Pharmacia (Uppsala, Sweden). The glass microfiber filters (GF/C Whatman) were purchased from Tamar (Jerusalem, Israel). The Chelex 100 was obtained from Bio-Rad (USA). $^{45}CaCl_2$ (10–30 mCi/mg) was purchased from DuPont NEN (Boston, MA) or Perkin Elmer (Monza, Italy). Fluo-4 ($K_5$) and fluo-3 AM were from Teflabs (Austin, TX, USA), Biotium (Toronto, Canada) or Molecular Probes (Eugene, OR, USA). The following reagents were used for preparing cardiomyocytes: Penicillin streptomycin (Biological Industries, Haemek, Israel), Bovine calf serum (Hyclone, USA), collagenase II (Worthington, NG, USA), trypsin, minimal essential medium-1 and L-glutamine (Gibco Invitrogen, Scotland). The scintillation cocktail Opti-Fluor was from Packard (Groningen, The Netherlands). All other reagents were analytical or HPLC grade. Deionized water (18 MegaOhms/cm, Millipore system) was used for preparing solutions.

### Effect of $NCX_{IF}$ on $Na_i$-dependent $^{45}Ca$ uptake in sarcolemma vesicles

The sarcolemma vesicles were obtained according to established procedures (27,28). The $Na_i$-dependent $^{45}Ca$ uptake was initiated by rapid dilution of Na-loaded vesicles in an assay medium containing $^{45}Ca$ with lipid/protein-free aliquots of $NCX_{IF}$ (17–21). The inhibitory capacity of $NCX_{IF}$ preparations was quantitatively evaluated in arbitrary inhibitory units (one inhibitory unit represents the amount of $NCX_{IF}$ that inhibits the $Na_i$-dependent $^{45}Ca$-uptake by 1% under fixed experimental conditions) (17–23). The samples can be stored at −70°C without any loss of inhibitory activity of $NCX_{IF}$ at least for 8–12 months.

### Extraction and pre-column purification of $NCX_{IF}$

$NCX_{IF}$ was extracted from 6–8 kg calf ventricle muscle with 95% ethanol, as previously described (17–23). Briefly, after ethanol was evaporated, the remaining aqueous phase was reduced to 0.3–0.5 L and insoluble material was removed by centrifugation (20,000 × g for 30 min). From the supernatant, lipids were removed by chloroform, and cold ethanol (−20°C) was added to the aqueous phase (to yield ~ 80%). White precipitate was removed by centrifugation and after ethanol was evaporated, cold acetone was added to yield ~ 90%. White precipitate was removed by centrifugation and concentrated material (100–150 ml) was passed through equal volumes of Dowex 2 × 8 (acetate form) and Dowex 50W ($H^+$ form) slurry. The collected effluents were reduced to 50–80 ml (yellow-brown color) and then passed through the CarbPacking SPE (60 ml/10gr) cartridge (Supelco, Bellefonte, USA). The nearly colorless effluent (30–50 ml) was loaded onto the Sephadex G-10 column (5.5 × 70 cm) and flashed with water (2 ml/min). The fractions containing the $NCX_{IF}$ activity were concentrated, filtrated, and stored at −70°C until purified further (17,18).

### Chromatography

Fully computerized HPLC systems were used for $NCX_{IF}$ purification, as described in previous publications (18–23). A combination of RP- and HILIC HPLC columns was used in the present work for $NCX_{IF}$ purification: The Synergi Polar (Phenomenex, USA, 250 × 21 mm, 4 μm), TSK-gel Amide-80 (TosoHaas, Ltd. Japan, 21 × 300 mm, 7 μm), Krumasil

Silica 100A (Phenomenex, USA, 250 × 21.2 mm, 5 μm), apHera-$NH_2$ (Astec, USA, 250 × 4.6 mm, 5 μm), Cyclobond I 2000, β-cyclodextran (Astec, USA, 250 × 4.6 mm, 5 μm), ZIC-*p*HILIC (SeQuant, Sweden, 150 × 4.6 mm, 5 μm) and Aminex HPX-87c (250 × 4 mm, 9μm). For HILIC columns, the injecting samples were dissolved in 80–95% methanol. All HPLC columns were run at 22–25°C, besides the Aminex column, which was explored at 60–80°C.

## Preparation of cardiomyocytes

Isolated ventricular myocytes were obtained from adult female Sprague-Dawley rats (225–250 gr). Briefly, rats were deeply anesthetized with sodium pentobarbital (0.1 mg/gr ip) and heparinized (1.25 U/gr ip). Fifteen min after heparin was injected, the heart was rapidly excised and rinsed with cold 250 μM EGTA isolation buffer containing (in mM): 130 NaCl, 1 lactic Acid, 5.4 KCl, 3 Na-pyruvate, 25 HEPES, 0.5 $MgCl_2$, 0.33 $NaH_2PO_4$, 22 D-Glucose, 0.01 u/ml Insulin, at pH 7.4 (adjusted with NaOH). The aorta was quickly cannulated for Langendorff perfusion. The heart coronary arteries were perfused at 37° C for 2 min with EGTA isolation buffer, and then perfused for 8 minutes with the same buffer supplemented with 50 μM $CaCl_2$, 1.6 mg/ml Collagenase (type II; Worthington Biochemical, Lakewood, NJ), and 0.04 mg/ml Protease (XIV). The ventricles were cut down, minced, and then gently agitated for 4 min in isolation buffer containing 83 μM $CaCl_2$, 1 mg/ml collagenase, 0.066 mg/ml Protease, and 1.66% BSA. The cells were filtered through nylon mesh (300 μm), and after having been washed, were resuspended, in succession, in enzyme-free isolation buffer (1% BSA) containing 250 μM and 500 μM $CaCl_2$. After a final wash, the cardiomyocytes were resuspended at room temperature in the cell media (17.4 mg/ml HEPES-buffered DMEM) supplemented with 10% fetal calf serum (Gibco), 0.01 u/ml insulin, and 44 mM NaCl, at pH 7.4 (adjusted with NaOH).

## Simultaneous measurements of $I_{NCX}$ and $[Ca]_i$ by patch-clamp and confocal microscopy

A patch-clamp method was combined with confocal $Ca^{2+}$ imaging microscopy to enable simultaneous measurement of $I_{NCX}$ and $[Ca]_i$ recordings in single cardiomyocytes exposed to a sub-maximal but high level (5 mM) of caffeine (24–26) To this end, freshly isolated cardiomyocytes were attached to laminin-coated coverslips and used within 4–5 h. Only quiescent, rod-shaped myocytes with clear striations were used. Experiments were performed at room temperature (20–23°C). The Giga-Ohm seal was attained while superfusing the recording chamber with normal Tyrode containing (in mM): 140 NaCl, 10 D-glucose, 2 $CaCl_2$, 10 HEPES, 1 $MgCl_2$, 4 KCl, at pH 7.4 (adjusted with NaOH). The patch pipette (1.8–2.2-M′Ω) was filled with a solution that contained (in mM): 2.5 $Na_2ATP$, 2.5 MgATP, 2.5 $MgCl_2$, 30 KCl, 110 K-aspartic acid, 10 HEPES, 0.05 Fluo-4 $K_5$ (molecular probes), at pH 7.2 (adjusted with KOH). After the whole-cell patch clamp was established, the cells were superfused with normal Tyrode supplemented with 5mM 4-aminopyridine, and 0.1mM $BaCl_2$. Cells were loaded for 8–10 minutes with fluo-4 through the patch pipette before the experiments were started. Voltage control and recordings were performed with an Axopatch 200A amplifier and Digidata 1322A (Axon Instruments). Currents were low-pass filtered at 1 kHz and sampled at 2 kHz. All currents were normalized to cell capacitance to account for differences in cell size, and data are reported as current densities (pA/pF). Cell capacitance was calculated from the capacity transient elicited by 10-ms hyperpolarization pulses from −90 to −95mV. To elicit $I_{NCX}$, the patched cardiomyocyte was held at −80 mV and 5-mm Caffeine (5 mM) was locally applied for 5 sec by a Pneumatic Pico Pump (PV830, World Precision Instruments, Inc.). $[Ca]_i$ imaging was performed with a Zeiss (LSM510) laser scanning confocal microscope equipped with an argon laser and a 63X 1.4 NA oil immersion objective (Zeiss). The scanned line was positioned along the longitudinal axis of the cardiomyocyte, fluo-4 was excited at 488 nm, and the fluorescence above 505 nm was recorded. Line-scan images (time vs. x) were acquired at a sampling rate of 1.92 ms per

line. Caffeine application was repeated every 7 min for as long as the cardiomyocytes remained quiescent; the leak currents were stable and under 200 pA. In order to keep the cardiomyocytes undamaged due to the caffeine exposure, 5 mM caffeine concentrations were used in all experiments.

### Detection of the $Ca^{2+}$-entry and $Ca^{2+}$-exit modes of NCX1 in single cardiomyocytes

The forward and reverse modes of NCX1 were measured in fluo-3-loaded rat cardiomyocytes, according to established protocols (33,34). In these experiments, the SR function was completely blocked by pretreatment of cardiomyocytes with 10 μM ryanodine and 1 μM thapsigargin. To assess the $Ca^{2+}$ entry via NCX1, we abruptly replaced the extracellular NaCl (137 mM) by the same concentration of TMA for 20 sec. The $Ca^{2+}$ exit mode was induced by replacing 137 mM TMA with 137 mM NaCl. The $[Ca^{2+}]_i$ in cardiomyocytes was detected with fluo-3 by using wide-field fluorescence microscopy (22). The prepared cover slips, containing fluo-3-loaded cardiomyocytes, were placed in a recording chamber on the stage of an inverted microscope (Olympus IX-71, Japan). The chamber was perfused with the following (in mM): NaCl 137, KCl 4, $MgSO_4$ 1.2, Glucose 10, HEPES 10, and $CaCl_2$ 1.5 (pH 7.4) at 27°C with a temperature controller system (Automatic Temperature Controller, TC-324B, Warner). The excitation light (mercury burner, 100W, Osram) was passed through a set of neutral density and excitation filters (HQ480, Chroma) and focused by a 40X objective (LCPlanF1, Olympus) and field diaphragm (allowing full illumination of single cardiomyocytes). Next, the emitted fluorescence was filtered through the dichroic mirror (Q505LP, Chroma, USA) and emission filter (HQ535, Chroma, USA). The fluorescence signal was recorded with a photon counting device (C&L Instruments, USA), and digitized by a PCI-DAQ card. Each experiment was recorded and stored as a separate file by using Chart v.4.12 software (ADInstruments, Australia). After subtraction of auto fluorescence, the fluo-3-recorded signal was calibrated to $[Ca]_i$ values according to a pseudo-ratio equation. It was assumed that the $K_d$ value for fluo-3 is 650 nM at 27°C and that resting $[Ca]_i$ is 100 nM, before the cells were treated with thapsigargin and ryanodine.

### Fluo-4 calibration

In the confocal microscopy experiments, the average fluorescence per pixel in a scanned line was taken as the observed fluorescence. Before a cardiomyocyte was patched, its auto-fluorescence was measured under the same scanning conditions as in the following experiment. The F value was taken after subtracting the auto fluorescence. Since the emission of fluo-4 is negligible in the absence of Ca ($F_{min} \sim 0$), the $[Ca^{2+}]_i$ was calculated as $[Ca^{2+}]_i = K_d \cdot (F)/(F_{max} - F)$. $F_{max}$ was measured directly from each cardiomyocyte at the end of the experiment, as previously outlined (24,25).

### Miscellaneous assays

Protein was measured by using a modified method of Lowry (35). Fluorescamine was used for detecting the α-amines and peptides (36). Reducing sugars were detected with phenol-sulfuric acid reagent (37). All analytical assays were downscaled for microplate measurements.

### Statistics

All data are presented as mean ± SEM. Statistical analysis was done by using the Two Sample t-Test (Origin 7.0, Northampton MA, USA). P values less than 0.05 were considered to be significant.

## Results

### HPLC procedures for $NCX_{IF}$ purification

The previous purification procedures of $NCX_{IF}$ suffered from inadequate pure separation quality, low loading capacity, and unsatisfactory levels of final yield (17,18). A new set of advanced HILIC columns was introduced to overcome these problems. The new purification scheme is based on combining new preparative (Krumasil-Silica) and analytic (ZIC-HILIC and Hypera) HILIC columns with previously explored preparative columns (RP Synergi-Polar and TSK-Amide 80) (Fig. 1). The new purification scheme provides a final yield of ~0.03 mg $NCX_{IF}$ per kg of starting material, which is at least 3–4 times higher than the highest yields obtained in previous preparations (17–23). A major reason for this improvement is the efficacy of the new HILIC columns, Krumasil-Silica (Fig. 1B), ZIC-HILIC (Fig. 1D), and Hypera (Fig. 1E). Despite this progress, currently available quantities of purified $NCX_{IF}$ are still not enough for structural studies by 2D NMR.

The Aminex column is an excellent matrix for separating disaccharide, hexose, and pentose structures. Therefore, an attempt was made to compare the retention time of purified $NCX_{IF}$ to known molecular “witnesses” in order find any possible correlation between the chromatographic behavior of $NCX_{IF}$ and its chemical structure. The inhibitory activity of $NCX_{IF}$ is eluted as a single peak, while showing a complete overlap (in time) with optical signals recorded at short UV (Fig. 2). In general, this kind of overlap of optical signals with inhibitory activity refers to the high quality of the purified substance. Eluted fractions of active $NCX_{IF}$ (Fig. 2) exhibit no chemical reactivity with fluorescamine or phenol-sulfur reagent (see Materials and Methods), thereby suggesting no content of the primary amine or aldehyde groups in the purified preparations of $NCX_{IF.}$ The chromatographic properties of $NCX_{IF}$ were compared with “witness” molecules (mono-, di-, tri-, and tetra-saccharides) by using the advanced HILIC-HPLC columns. The retention time of $NCX_{IF}$ on the ZIC-HILIC (Fig. 1D) and Aminex (Fig. 2) columns is characteristic of disaccharide-sized molecules. Attempts at structural analysis by LC/MS were not successful due to the extremely weak ionization ability of $NCX_{IF}$.

### Effect of $NCX_{IF}$ on the $Ca^{2+}$-entry and $Ca^{2+}$-exit modes of the $Na^+/Ca^{2+}$ exchanger in intact cardiomyocytes

The $Ca^{2+}$-entry and $Ca^{2+}$-exit modes of NCX1 were monitored in intact cardiomyocytes under conditions at which the SR $Ca^{2+}$ fluxes were completely blocked by pretreatment of cardiomyocytes with ryanodine and thapsigargin (33,34). To assess the $Ca^{2+}$-entry via NCX1, extracellular $Na^+$ was abruptly removed (replaced by TMA) for 20 sec and $Ca^{2+}$ entry was monitored by measuring changes in $[Ca^{2+}]_i$ using fluo-3. Figure 3A shows that $Na^+$ removal results in the elevation of $[Ca^{2+}]_i$ (net $Ca^{2+}$-entry). Following the removal of extracellular $Na^+$, the return of extracellular $[Na]_o$ to normal levels resulted in decreased $[Ca^{2+}]_i$ and reflects the net exit of $Ca^{2+}$ via the $Na^+/Ca^{2+}$ exchanger. Two consecutive series of $Na^+$-abrupt episodes in the same cardiomyocyte (separated by 5 minutes) produced comparable changes in the amplitude and rates of the $[Ca^{2+}]_i$ (Fig. 3A). Therefore, the inhibitory effects of $NCX_{IF}$ can be reliably evaluated in the same cardiomyocyte during the second $Na^+$-abrupt episode (the first $Na^+$-abrupt can be used as a control). The bidirectional $Ca^{2+}$-fluxes through NCX1 were examined by transient superfusion of cadiomyocytes with extracellular $NCX_{IF}$ (50 units/ml for 5 min). $NCX_{IF}$ significantly reduced the rate and magnitude of the changes in $[Ca^{2+}]_i$ (Fig. 3B). $NCX_{IF}$ results in a slowing of the rate of $Ca^{2+}$-entry and of the $Ca^{2+}$-exit (Fig. 3C). Moreover, $NCX_{IF}$ reduces the amplitude of $[Ca^{2+}]_i$ elevation (to 15.0 ± 4.8% of the control, $p < 0.001$) and decreases the rate of $Ca^{2+}$-entry (11.9 ± 7.2% of the control, $p < 0.001$) and of $Ca^{2+}$-exit (5.6 ± 2.2% of the control, $p < 0.0001$) (Fig. 3D). Therefore, $NCX_{IF}$ can effectively inhibit both the $Ca^{2+}$-entry and $Ca^{2+}$-

exit modes of NCX1 in intact cardiomyocytes, as expected, based on transport thermodynamics (50,51). These properties of $NCX_{IF}$, which can comparably alter both the $Ca^{2+}$-entry and Ca2+-exit modes of NCX1, seem to be very different from the properties of the synthetic NCX-blocker, KB-R7943, which exhibits a preferential selectivity for inhibiting the $Ca^{2+}$-entry mode in a single cardiomyocyte system (33,38).

Although the $Na^{+}$-abrupt protocol enables to assess the $Ca^{2+}$-entry and $Ca^{2+}$-exit modes of NCX1 in intact single cell, this method cannot resolve whether $NCX_{IF}$ interacts with the extracellular or intracellular domain. Therefore, the application of complementary approaches was necessary to resolve the side-ness of $NCX_{IF}$ action in intact cardiomyocytes (see below).

## Direct loading of $NCX_{IF}$ into the cytoplasm inhibits the $I_{NCX}$ and $Ca^{2+}$-extrusion in intact cardiomyocytes

To further investigate the sidedness of $NCX_{IF}$ interactions with NCX1, we carried out patch clamp experiments. Briefly, $NCX_{IF}$ was applied to the interior of intact cardiomyocytes through the patch pipette. In these experiments, $I_{NCX}$ was measured simultaneously with $[Ca^{2+}]_i$ using a combination of patch clamp and confocal microscopy. Under control conditions, application of caffeine (for 5sec) activates the release of SR $Ca^{2+}$ and elevates $[Ca^{2+}]_i$, consequently enhancing $Ca^{2+}$-activated inward $I_{NCX}$ current (24–26). In patched cardiomyocytes, the cytoplasm was equilibrated with pipette solution containing either no $NCX_{IF}$ (gthe control group) or 50 units/ml $NCX_{IF}$ (the $NCX_{IF}$ group). Figure 4A shows a typical recording obtained from either a control or from a cardiomyocyte loaded with 50 units/ml $NCX_{IF}$. The $[Ca^{2+}]_i$ transient, induced by caffeine, was significantly higher in the $NCX_{IF}$-loaded myocytes (1.66 ± 0.35 μM, n=16) than in the control group without $NCX_{IF}$ (0.34 ± 0.1 μM, n=10; $p < 0.01$), as shown in Fig. 4. The peak $I_{NCX}$ value was insignificantly lower in $NCX_{IF}$-loaded cardiomyocytes, 0.61 ± 0.05 pA/pF than in the control group, 0.79 ± 0.20 pA/pF (data not shown). As shown in Fig. 4B, the $I_{NCX}$ per $\Delta[Ca^{2+}]_i$ is much greater in controls than in the presence of $NCX_{IF}$. Therefore, a given concentration of cytosolic $NCX_{IF}$ significantly blocks NCX1 in a single cardiomyocyte system.

## Effect of $NCX_{IF}$ on the $I_{NCX}/[Ca]_i$ relationship

The dependence of $I_{NCX}$ on $[Ca^{2+}]_i$ can be measured dynamically during the time when the application of caffeine increases $[Ca^{2+}]_i$ and its removal leads to the fall of $[Ca^{2+}]_i$. The data analysis was established by plotting $I_{NCX}$ during the elevation of $[Ca^{2+}]_i$, as shown in Fig. 5 and its fall, as shown in Fig. 6. Intracellular $NCX_{IF}$ reduces $I_{NCX}$ at any $[Ca^{2+}]_i$ value, consistent with the NCX1 block. The data fitted by linear regression clearly indicates that the slope of $I_{NCX}$ vs. $[Ca^{2+}]_i$ is less steep (~6-fold) in $NCX_{IF}$-loaded cardiomyocytes, than in control cardiomyocytes in the absence of $NCX_{IF}$. The cytosolic $NCX_{IF}$ has very similar effects on the $I_{NCX}/[Ca^{2+}]_i$ slope during the raising (6.0 ± 0.02-fold change in the slope, Fig. 5B) or the decay phase (5.94 ± 0.02-fold change in the slope, Fig. 6B) of caffeine-induced $[Ca^{2+}]$-transient. The present data clearly indicate that $NCX_{IF}$ inhibits both the NCX-mediated inward current and $[Ca^{2+}]$-extrusion from the cell in a comparable way.

At fixed doses of $NCX_{IF}$, the fraction of $I_{NCX}$ inhibition is independent of $[Ca^{2+}]_i$, at least in the tested range of $[Ca^{2+}]_i$ = 30–2500 μM (Figs. 5 and 6). This observation provides independent evidence that the degree of inhibition is determined by $NCX_{IF}$ dose and not by $[Ca^{2+}]_i$. As a precaution, one has to take into account that under the experimental conditions tested here, the regulatory sites of NCX1 are fully saturated by cytosolic $Ca^{2+}$. Therefore, a more extensive investigation is required for testing the effects of $NCX_{IF}$ on $Ca^{2+}$ interaction with the CBD1 and CBD2 domains.

## Discussion

Purification procedures developed in our laboratory (17,18) permitted primary characterization of $NCX_{IF}$ properties (17–23), although these preparations still suffer from weak chromatographic resolution, inadequate pure loading capacity, and low yield. Since milligram quantities of purified $NCX_{IF}$ are required for structural studies, here we describe further improvements in the purification procedures. Although our previous work provided accumulating evidence for the $NCX_{IF}$-induced inhibition of NCX1 activities *in vitro* (17–19) and for the modulation of muscle contractility (17,20–23), there was no evidence for inhibition of NCX1 in the single-cell system. Therefore, the present work represents the first attempt at measuring the direct actions of $NCX_{IF}$ on the $Na^+/Ca^{2+}$ exchanger activities in a single-cell system by performing simultaneous measurements of $I_{NCX}$ and cytosolic $[Ca^{2+}]_i$. As predicted from thermodynamic considerations, $NCX_{IF}$ blocks equally well both $Ca^{2+}$ extrusion and $Ca^{2+}$ entry modes of NCX1. It appears that $NCX_{IF}$ acts effectively from the cytosolic side, exhibiting an inhibitory potency that is comparable with the inhibitory potency observed previously with *in vitro* systems of isolated sarcolemma vesicles (17–20). Some issues related to the characteristics of $NCX_{IF}$ action are discussed below.

### Characteristic properties of purified $NCX_{IF}$ preparations

A several-fold increase in the yield of purified $NCX_{IF}$ preparations were obtained by introducing new HILIC technologies at various stages of the purification scheme (Fig. 1). Despite a significant improvement in preparative procedures, the available amounts of purified $NCX_{IF}$ are still not enough to elucidate the $NCX_{IF}$ structure by 2D NMR. To obtain sufficient (milligram) quantities of $NCX_{IF}$ for structural analysis by NMR, one has to scale-up the existing purification procedures at least 5–10-fold (with starting material of 40–50-kg ventricles). Unfortunately, these near-industrial procedures for purification could not be handled in the present work due to the lack of available resources.

Another principal problem in molecular identification of $NCX_{IF}$ is that the *de novo* identification of unknown substances by MS-techniques depends on the chemical nature of the investigated substance (39,40). For example, small charged molecules (e.g., such as peptides) can be successfully analyzed even at $10^{-9}$ M, whereas the analysis of hydrophilic, uncharged molecules (e.g., such as small polyols) could be a challenge even at $10^{-3}$ M (39–41). If $NCX_{IF}$ is a hydroxyl-rich compound (as we suspect) this would explain why it is so difficult to resolve its structure by MS techniques. Consistent with our previous findings (18), $NCX_{IF}$ exhibits very weak absorption only in the short UV (190–200 nm) range (Fig. 2), thereby suggesting that neither aromatic rings (nucleotides, phenols, indols, etc.) nor conjugated chemical groups are present. In agreement with previous analyses (17,18), purified $NCX_{IF}$ (Fig. 2) does not react with fluorescamine or phenol-sulfur reagents. Therefore, there is no evidence that $NCX_{IF}$ contains primary amine or aldehide groups. In potential, the covalent modification of putative hydroxyl groups of $NCX_{IF}$ may enhance the MS and/or NMR signals by an order of magnitude but unfortunately, due to the extremely low solubility of $NCX_{IF}$ in organic solvents (even in pyridine), the chemical modification of hydroxyl group(s) is also not a trivial task.

### $NCX_{IF}$ inhibits both the $Ca^{2+}$-entry and $Ca^{2+}$-exit modes of NCX1 in intact cardiomyocytes

Although the synthetic NCX blocker KB-R7943 has been reported to preferentially block the $Ca^{2+}$ entry mode of NCX1 in isolated cardiac myocytes (33,38), this explanation is unsatisfactory (42), given the requirements of thermodynamics (50,51). This may be explained by the fact that experimental conditions are not sufficiently comparable in the KB-R7943 studies. Here, the conditions for examining both modes of NCX1 action were nearly identical when $NCX_{IF}$ was used to block NCX1. $NCX_{IF}$ blocks equally well for both the

$Ca^{2+}$ entry and $Ca^{2+}$ exit modes of NCX1, as shown in Figure 3. Moreover, $NCX_{IF}$ alters not only the rates of $Ca^{2+}$ entry/exit modes but also the rate constants of both modes (Fig. 3B). These data suggest that $NCX_{IF}$ may alter the turnover rate constant of the exchange cycle by affecting the rate-limiting step of net ion transport. This is in a good agreement with previous results (21), suggesting that $NCX_{IF}$ affects the rate-limiting step of ion-translocation without interfering with the ion-binding at the transport site(s) of NCX1.

## Cytosolic $NCX_{IF}$ inhibits the NCX1-mediated ion currents at any given $[Ca^{2+}]_i$

$NCX_{IF}$ was directly loaded into the cytoplasm of patched cardiomyoctes in order to investigate the sidedness of $NCX_{IF}$ action. Inward $I_{NCX}$ was activated by elevation of $[Ca^{2+}]_i$ following transient exposure to caffeine. Simultaneous monitoring of $I_{NCX}$ and $[Ca^{2+}]_i$ has shown that intracellular $NCX_{IF}$ reduces $I_{NCX}$ at any given $[Ca^{2+}]_i$ (Figs. 5 and 6). At fixed doses of $NCX_{IF}$, the fraction of $I_{NCX}$ inhibition is independent of $[Ca^{2+}]_i$ (Figs. 5 and 6), suggesting that the extent of inhibition is controlled by $NCX_{IF}$ dose and not by cytosolic $Ca^{2+}$ level. The significance of the present findings is that $NCX_{IF}$ may interact with some specific cytosolic domain to inhibit NCX1. Notably, the regulatory sites of NCX1 are fully saturated by cytosolic $Ca^{2+}$ under the experimental conditions tested here (Figs. 5 and 6). Therefore, the future testing of $NCX_{IF}$ for its capacity to affect the $Ca^{2+}$ interactions with the CBD1 and CBD2 domains is highly encouraging.

The present experiments clearly demonstrate that $NCX_{IF}$ can be effectively “entrapped” inside the cell by direct loading of $NCX_{IF}$ into the cytoplasm of patched cardiomyocyte (Figs. 4–6). Although unproven, it seems plausible that an extracellular site of action is unlikely since the extracellular concentration would be significantly reduced by dilution following intracellular administration. In contrast, the extracellular application of $NCX_{IF}$ would tend to load the cell with the inhibitor if it should leak (transport) in, as we suspect it does. This would then explain the efficacy of extracellular application of $NCX_{IF}$ in the present experiments describing the bidirectional inhibition of NCX1 (Figure 3). In the absence of $NCX_{IF}$ breakdown, extracellular application of $NCX_{IF}$ should lead to steady-state levels of intracellular $NCX_{IF}$ approaching the extracellular concentration.

## Brief comparison of $NCX_{IF}$ with existing NCX-blockers

A considerable amount of work has been devoted to the development of peptide (27–32, 42–44) and organic (38,45–47) NCX-blockers; however, all of them have some specific, but principal drawbacks. For example, the synthetic blockers (KB-R7943, SEA-0400, and SN-6) inhibit not only NCX, but also the other ion-transport systems (38,48). Another principal drawback is the enigmatic putative preferential inhibition of the $Ca^{2+}$-entry mode, which would appear to limit its pharmacological significance and utility (33,49). In contrast to the organic NCX-blockers, XIP and FRCRCFa can effectively inhibit both the inward and outward currents of NCX by interacting with the cytosolic domain (42–44), but these blockers are inactive when added extracellularly due to their impermeability to the cell membrane.

In contrast to the synthetic blocker, KB-R7943, $NCX_{IF}$ results in a comparable inhibition of both the $Ca^{2+}$-entry and $Ca^{2+}$-exit modes in intact cardiomyocytes (Fig. 3). Although KB-R7943 and $NCX_{IF}$ are both active when added outside the cell, the striking difference is that KB-R7943 interacts with the extracellular domain, whereas $NCX_{IF}$ might approach the cytosolic site in order to inhibit NCX1 (Figs 5 and 6). More extensive research is required for comparing $NCX_{IF}$ with the more recently developed NCX-inhibitors, SEA0400 and SN-6.

## Acknowledgments

This work was funded by the USA-Israeli Binational Foundation, Research Grant # 2003-372 (DK and WJL), Israeli Ministry of Health, Research Grant # 3000003019 (DK), NIHLBI, and MBC-UMBI initiative funds (WJL). The Ph.D. stipend of LB was supported by the Dr. Miriam and Sheldon G. Edelson Foundation.

## Abbreviations

| | |
|---|---|
| **Arsenazo III** | 2,2′-(1,8-dihydroxy-3,6-disulfonaphthylene-2,7-bisazo)bisbenzenearsonic acid |
| **Fluo-3** | N-[2-[2[bis(carboxymethyl)amino]-5-(2,7dichloro-6-hydroxy-3-oxy-3H-xanthen-9-yl) henoxy]ethoxy]-4 methylphenyl]-N-(carboxymethyl)glycine |
| **Fluorescamine** | 4-Phenylspiro[furan-2(3H),1′-phthalan] 3,3-dione |
| **FRCRCFa** | the S-S bond cyclic hexapeptide Phe-Arg-Cys-Arg-Cys-Phe-$NH_2$ |
| **XIP** | the inhibitory peptide containing twenty amino acids |
| **LC/MS** | Liquid chromatography coupled with mass-spectroscopy |
| **LC/MS/MS** | Liquid chromatography coupled with MS/MS |
| **Mops** | 3-(N-morpholino)propanesulfonic acid |
| **Tris** | tris(hydroxymethyl)aminomethane |
| **PMSF** | Phenylmethanesulfonyl fluoride |
| **TMA** | tetramethylammonium |

## References

1. Carafoli E. Intracellular calcium homeostasis. Ann Rev Biochem. 1987; 56:395–433. [PubMed: 3304139]
2. Philipson KD, Nicoll DA. Sodium-calcium exchange: a molecular perspective. Annu Rev Physiol. 2000; 62:111–133. [PubMed: 10845086]
3. Blaustein MP, Lederer WJ. Sodium/calcium exchange: its physiological implications. Physiol Rev Physiol Rev. 1999; 79:763–854.
4. Khananshvili, D. Structure, mechanism and regulation of the Cardiac Sarcolemma $Na^+$-$Ca^{2+}$ Exchanger. In: Anderson, JP., editor. Adv Molec & Cell Biol Life Sciences Program. Vol. 23B. JAI Press, Inc; 1998. p. 309-356.
5. Kofuji P, Lederer WJ, Schulze DH. Mutually exclusive and cassette exons underlie alternatively spliced isoforms of the Na/Ca exchanger. J Biol Chem. 1994; 269:5145–5149. [PubMed: 8106495]
6. Lee SL, Yu AS, Lytton J. Tissue-specific expression of $Na^+$-$Ca^{2+}$ exchanger isoforms. J Biol Chem. 1994; 269:14849–14852. [PubMed: 8195112]
7. Quednau BD, Nicoll DA, Philipson KD. Tissue specificity and alternative splicing of the $Na^+$/$Ca^{2+}$ exchanger isoforms NCX1, NCX2, and NCX3 in rat. Am J Physiol. 1997; 272:C1250–1261. [PubMed: 9142850]
8. Reeves JP, Hale CC. The stoichiometry of the cardiac sodium-calcium exchange system. J Biol Chem. 1984; 259:7733–7739. [PubMed: 6736024]
9. Pogwizd SM, Schlotthauer K, Li L, Yuan W, Bers DM. Arrhythmogenesis and contractile dysfunction in heart failure: roles of sodium-calcium exchange, inward rectifier potassium current and residual β-adrenergic responsiveness. Circ Res. 2000; 88:1159–1167. [PubMed: 11397782]
10. Matsuoka S, Nicoll DA, Reilly RF, Hilgemann DW, Philipson KD. Initial localization of regulatory regions of the cardiac sarcolemmal $Na^+$-$Ca^{2+}$ exchanger. Proc Natl Acad Sci USA. 1993; 90:3870–3874. [PubMed: 8483905]

11. Di Polo R, Beauge L. Ionic ligand interactions with the intracellular loop of the sodium-calcium. Modulation by ATP. Prog Biophys Mol Boil. 2002; 80:43–67.
12. Doering AE, Eisner DA, Lederer WJ. Cardiac Na-Ca exchange and pH. Ann NY Acad Sci USA. 1995; 779:182–198.
13. Bers DM, Ginsburg KS. Na:Ca stoichiometry and cytosolic Ca-dependent activation of NCX in intact cardiomyocytes. Ann N Y Acad Sci. 2007; 1099:326–338. [PubMed: 17303827]
14. Hilge M, Aelen J, Vuister GW. $Ca^{2+}$ regulation in the $Na^{+}$-$Ca^{2+}$ exchanger involves two markedly different $Ca^{2+}$ sensors. Mol Cell. 2006; 22:15–25. [PubMed: 16600866]
15. Nicoll DA, Sawaya MR, Kwon S, Cascio D, Philipson KD, Abramson J. The crystal structure of the primary $Ca^{2+}$ sensor of the $Na^{+}/Ca^{2+}$ exchanger reveals a novel $Ca^{2+}$ binding motif. J Biol Chem. 2006; 281:21577–21581. [PubMed: 16774926]
16. Besserer G, Ottolia M, Nicoll DA, Chaptal V, Cascio D, Philipson KD, Abramson J. The second $Ca^{2+}$-binding domain of the $Na^{+}$-$Ca^{2+}$ exchanger is essential for regulation: Crystal structures and mutational analysis. Proc Nat Acad Sci U S A. 2007; 104:18467–18472.
17. Hiller R, Shpak C, Shavit G, Shpak B, Khananshvili D. An unknown endogenous inhibitor of Na/Ca exchange can enhance the cardiac muscle contractility. Biochem Biophys Res Com. 2000; 277:138–146. [PubMed: 11027654]
18. Boyman L, Hiller R, Shpak B, Yomtov E, Shpak C, Khananshvili D. Advanced procedures for separation and analysis of low molecular weight inhibitor ($NCX_{IF}$) of the cardiac sodium-calcium exchanger. Biochem Biophys Res Com. 2005; 337:936–943. [PubMed: 16226722]
19. Shpak C, Hiller R, Shpak B, Khananshvili D. The endogenous inhibitor of NCX1 does not resemble the properties of digitalis compound. Biochem Biophys Res Com. 2003; 308:114–119. [PubMed: 12890488]
20. Shpak B, Shpak C, Hiller R, Boyman L, Khananshvili D. Inotropic and lusitropic effects induced by the inhibitory factor of the Na/Ca exchanger are not mediated by the beta-adrenergic activation. J Cardiovasc Pharmacol. 2004; 44:466–472. [PubMed: 15454855]
21. Shpak C, Hiller R, Shpak B, Boyman L, Khananshvili D. The low molecular weight inhibitor of NCX1 interacts with a cytosolic domain that differs from the ion-transport site of the Na/Ca exchanger. Biochem Biophys Res Com. 2004; 324:1346–1351. [PubMed: 15504362]
22. Boyman L, Hiller R, Shpak B, Shpak C, Khananshvili D. Purified endogenous inhibitor of the Na/Ca exchanger can enhance the cardiomyocytes contractility and calcium transients. Biochem Biophys Res Commun. 2006; 346:1100–1107. [PubMed: 16782052]
23. Shpak B, Gofman Y, Shpak C, Hiller R, Boyman L, Khananshvili D. Effects of purified endogenous inhibitor of the $Na^{+}/Ca^{2+}$ exchanger on ouabain-induced arrhythmias in the atria and ventricle strips of guinea pig. Eur J Pharmacol. 2006; 553:196–204. [PubMed: 17078946]
24. Trafford AW, Diaz ME, Eisner DA. A novel, rapid and reversible method to measure Ca buffering and time-course of total sarcoplasmic reticulum Ca content ventricular myocytes. Plugers Arch. 1999; 437:501–503.
25. Diaz ME, Trafford AW, Eisner DA. The role of intracellular calcium buffers in determining the shape of the cytosolic Ca transient in cardiac ventricular myocytes. Plugers Arch. 2001; 442:96–100.
26. Pogwizd M, Sipido KR, Vendonck F, Bers DM. Intracellular Na in animal models of hypertrophy and heart failure: contractile function and arrhythmogenesis. Cardiovasc Res. 2003; 57:887–896. [PubMed: 12650867]
27. Khananshvili D, Shaulov G, Weil-Maslansky E, Baazov D. Positively charged cyclic hexapeptides, novel blockers for the cardiac sarcolemma $Na^{+}$-$Ca^{2+}$ exchange. J Biol Chem. 1995; 270:16182–16188. [PubMed: 7608184]
28. Khananshvili D, Mester B, Saltoun M, Shaulov G, Baazov D. Inhibition of the cardiac sarcolemma $Na^{+}$-$Ca^{2+}$ exchanger by conformationally constraint small peptides. Mol Pharmacol. 1997; 51:126–131. [PubMed: 9016354]
29. Khananshvili D. Distinction between the two basic mechanisms of cation transport in the cardiac $Na^{+}$-$Ca^{2+}$ exchange system. Biochemistry. 1990; 29:2437–2442. [PubMed: 2110471]

30. Khananshvili D, Shaulov G, Weil-Maslansky E. Rate-limiting mechanisms of exchange reactions in the cardiac sarcolemma $Na^+$-$Ca^{2+}$ exchanger. Biochemistry. 1995; 34:10290–10297. [PubMed: 7640285]
31. Khananshvili D, Baazov D, Weil-Maslansky E, Shaulov G, Mester B. Rapid interaction of FRCRCFa with cytosolic side of the cardiac sarcolemma $Na^+$-$Ca^{2+}$exchanger blocks the ion transport without preventing the binding of either sodium or calcium. Biochemistry. 1996; 35:15933–15940. [PubMed: 8961960]
32. Khananshvili D, Price DC, Greenberg MJ, Sarne Y. Phe-Met-Arg-Phe-$NH_2$ (FMRFa)-related peptides inhibit $Na^+$-$Ca^{2+}$ exchange in cardiac sarcolemma vesicles. J Biol Chem. 1993; 268:200–205. [PubMed: 8416928]
33. Satoh H, Ginsburg KS, Qing K, Terada H, Hayashi H, Bers DM. KB-R7943 block of $Ca^{2+}$ influx via $Na^+$-$Ca^{2+}$ exchange does not alter twitches or glycoside inotropy but prevents $Ca^{2+}$overload in rat ventricular myocytes. Circulation. 2000; 101:1441–1446. [PubMed: 10736290]
34. Li SZ, Wu F, Wang B, Wei GZ, Jin ZX, Zang YM, Zhou JJ, Wong TM. Role of reverse mode Na $^+$/$Ca^{2+}$ exchanger in the cardioprotection of metabolic inhibition preconditioning in rat ventricular myocytes. Eur J Pharmacol. 2007; 561:14–22. [PubMed: 17306252]
35. Markwell MA, Haas SM, Bieber LL, Tolbert NE. A modification of the Lowry procedure to simplify protein determination in membrane and lipoprotein samples. Anal Biochem. 1978; 87:206–210. [PubMed: 98070]
36. Udenfriend S, Stein S, Bohlen P, Dairman W, Leimgruber W, Weigele M. A reagent for assay of amino acids, peptides, proteins, and primary amines in the picomole range. Science. 1972; 178:871–872. [PubMed: 5085985]
37. Fox JD, Robyt JF. Miniaturization of three carbohydrate analyses using a microsample plate reader. Anal Biochem. 1991; 195:93–96. [PubMed: 1888021]
38. Iwamoto T, Watano T, Shigekawa M. A novel isothiourea derivative selectively inhibits the reverse mode of $Na^+$/$Ca^{2+}$ exchange in cells expressing NCX1. J Biol Chem. 1996; 271:22391–22397. [PubMed: 8798401]
39. Hemström P, Irgum K. Hydrophilic interaction chromatography. J Sep Sci. 2006; 29:1784–821. [PubMed: 16970185]
40. Zwiener C, Frimmel F. LC-MS analysis in the aquatic environment and in water treatment technology - a critical review. Part II: Applications for emerging contaminants and related pollutants, microorganisms and humic acids. Anal Bioanal Chem. 2004; 378:851–861. [PubMed: 14647937]
41. Cech NB, Enke CG. Practical implications of some recent studies in electrospray ionization fundamentals. Mass Spec Rev. 2001; 20:362–387.
42. Li Z, Nicoll DA, Collins A, Hilgemann DW, Filoteo AG, Penniston JT, Tomich JM, Philipson KD. Identification of a peptide inhibitor of the cardiac sarcolemmal $Na^+$-$Ca^{2+}$ exchanger. J Biol Chem. 1991; 266:1014–1020. [PubMed: 1985930]
43. Hobai IA, Khananshvili D, Levi AJ. The peptide 'FRCRCFa', dialyzed intracellularly, inhibits the Na/Ca exchange with high affinity in rabbit ventricular myocytes. Plugers Archiv. 1997; 433:455–463.
44. Meszaros J, Khananshvili D, Hart G. Mechanisms underlying delayed afterdepolarizations in hypertrophied left ventricular myocytes of the rat heart. Am J Physiol. 2001; 281:H903–H914.
45. Watano T, Kimura J, Morita T, Nakanishi H. A novel antagonist, No. 7943, of the $Na^+$/$Ca^{2+}$ exchange current in guinea-pig cardiac ventricular cells. Br J Pharmacol. 1996; 119:555–563. [PubMed: 8894178]
46. Matsuda T, Arakawa N, Takuma K, Kishida Y, Kawasaki Y, Sakaue M, Takahashi K, Takahashi T, Suzuki T, Ota T, Hamano-Takahashi A, Onishi M, Tanaka Y, Kameo K, Baba A. SEA0400, a novel and selective inhibitor of the $Na^+$-$Ca^{2+}$ exchanger, attenuates reperfusion injury in the in vitro and in vivo cerebral ischemic models. J Pharmacol Exp Ther. 2001; 298:249–256. [PubMed: 11408549]
47. Iwamoto T, Inoue Y, Ito K, Sakaue T, Kita S, Katsuragi T. The exchanger inhibitory peptide region-dependent inhibition of $Na^+$/$Ca^{2+}$ exchange by SN-6 [2-[4-(4-

nitrobenzyloxy)benzyl]thiazolidine-4-carboxylic acid ethyl ester], a novel benzyloxyphenyl derivative. Mol Pharmacol. 2004; 66:45–55. [PubMed: 15213295]

48. Reuter H, Henderson SA, Han T, Matsuda T, Baba A, Ross RS, Goldhaber JI, Philipson KD. Knockout mice for pharmacological screening: testing the specificity of $Na^+$-$Ca^{2+}$ exchange inhibitors. Circ Res. 2002; 91:90–92. [PubMed: 12142340]
49. Sipido KR, Varro A, Eisner D. Sodium calcium exchange as a target for antiarrhythmic therapy. Handb Exp Pharmacol. 2006:159–199. [PubMed: 16610344]
50. Noble D, Blaustein MP. Directionality in drug action on sodium-calcium exchange. Ann N Y Acad Sci. 2007; 1099:540–543. [PubMed: 17446499]
51. Ruknudin AM, Wei SK, Haigney MC, Lederer WJ, Schulze DH. Phosphorylation and other conundrums of Na/Ca exchanger, NCX1. Ann N Y Acad Sci. 2007; 1099:103–118. [PubMed: 17446449]

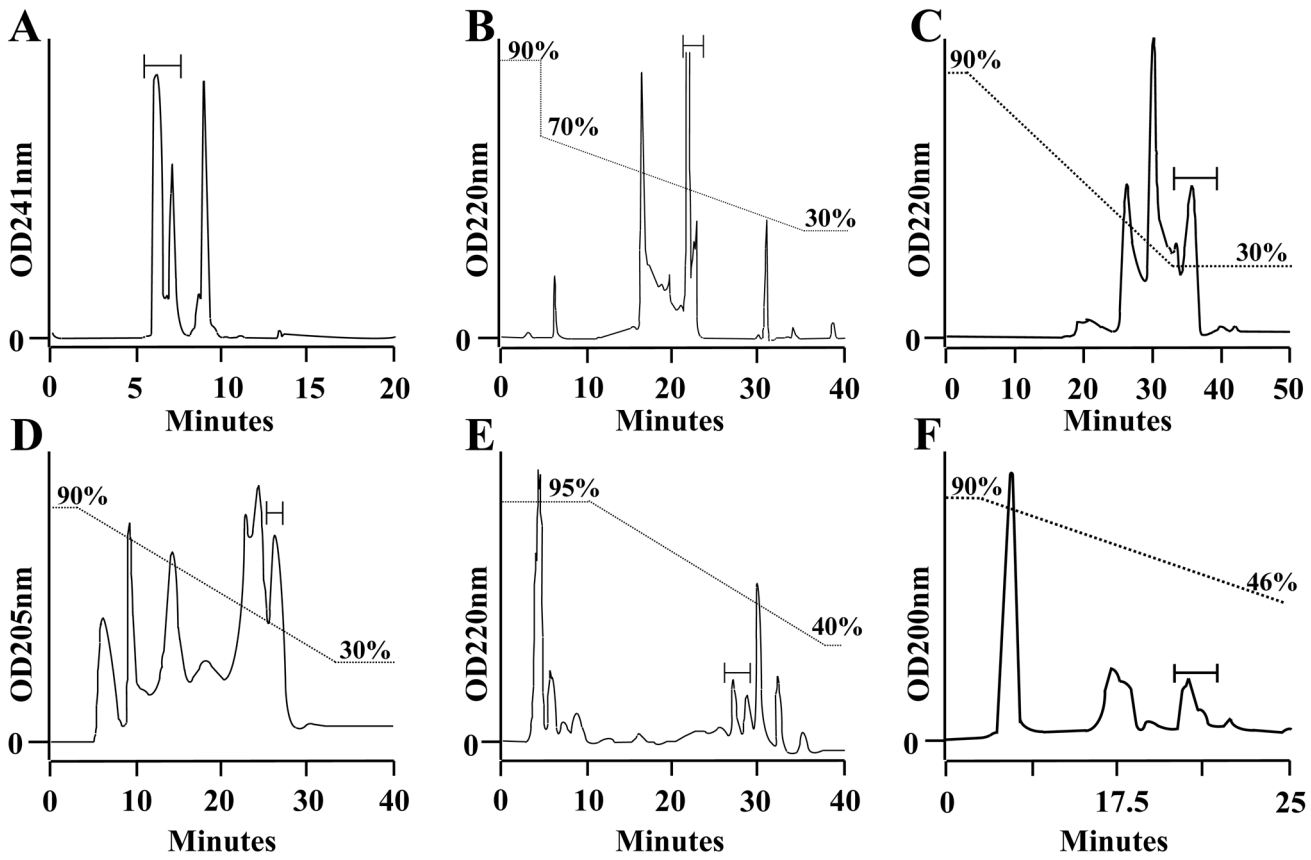


**Fig. 1. HPLC procedures for extensive purification of $NCX_{IF}$**

$NCX_{IF}$ was extracted and partially purified by solvent precipitation, gel-filtration, and ion-exchange procedures, as described in Materials and Methods. Partially purified $NCX_{IF}$ was further loaded on the HPLC columns in the following order: A. Synergi-Polar (10 ml/min). B. Krumasil-Silica (5 ml/min). C. TSK-gel Amide-80 (5 ml/min). D. ZIC-HILIC (0.5 ml/min). E. Hypera (1.0 ml/min). F. Cyclobond (1 ml/min). All other chromatographic conditions are described in Materials and Methods. Aliquots were removed from collected fractions, lyophilized, and then assayed for inhibition of the $Na^+/Ca^{2+}$ exchanger by using the standard assay of $Na_i$-dependent $^{45}Ca$-uptake in sarcolemma vesicles (see Materials and Methods). The active fractions obtained from 20–50 injections were pooled, lyophilized, and then the concentrated fractions were injected into the next column. Bars indicate the fractions containing the inhibitory activity of $NCX_{IF}$.

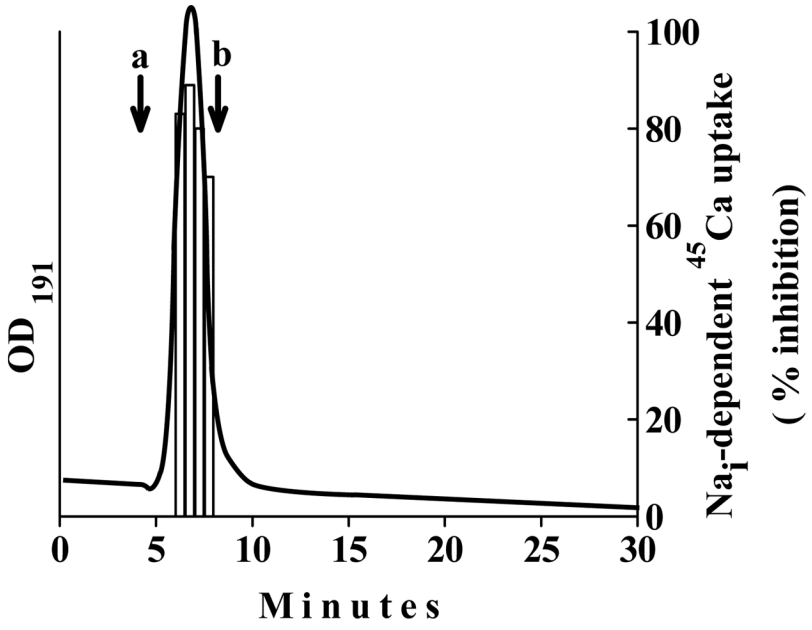


**Fig. 2. Comparison of the HPLC retention time of purified $NCX_{IF}$ with the mono- and disaccharide witnesses**

The active fractions of $NCX_{IF}$, obtained from the final step of purification (see Fig. 1), were loaded on the Aminex HPX-87c (250 × 4 mm, 9μm) and flashed with water (0.3 ml/min) at 60°C. Next, the fractions were tested for inhibitory activity of the $Na^+/Ca^{2+}$ exchanger by using the standard assay of $Na^+_i$-dependent $^{45}Ca$-uptake in isolated sarcolemma vesicles (see Materials and Methods). In control samples, the $Na^+/Ca^{2+}$ exchanger activity was assayed under the same experimental conditions with column effluent. Bars indicate the inhibition of $Na^+/Ca^{2+}$ exchanger activity. The straight line indicates continuous detection of effluent from the column at 191 nm. The *a* and *b* arrows indicate the retention times of glucose and sucrose, respectively (measured on the same column under the identical chromatographic conditions).

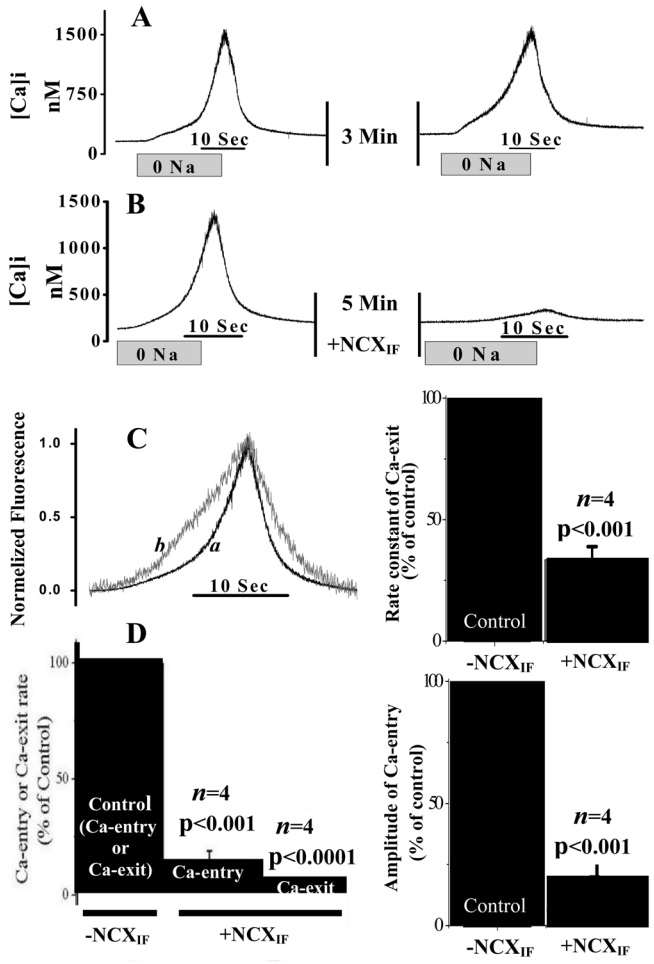


**Fig. 3. $NCX_{IF}$–dependent inhibition of $Ca^{2+}$-entry and $Ca^{2+}$-exit modes of the $Na^+/Ca^{2+}$ exchanger in intact cardiomyocytes**

The $Ca^{2+}$-entry and $Ca^{2+}$-exit modes of NCX were monitored in intact cardiomyocytes by perfusing the recording chamber with 0 mM $Na^+$ medium for 20 seconds (abrupt-0Na). Then the chamber was perfused with normal medium, as indicated, and subsequently, the second session of the $Ca^{2+}$-entry and $Ca^{2+}$-exit reaction was generated in the same cardiomyocyte by switching to the 0 mM $Na^+$ perfusion medium for 20 sec. ***A***. Two consecutive sections of $Na^+$-abrupt reaction in the absence of $NCX_{IF}$. ***B***. After the first abrupt-0 $Na^+$, the recording chamber was perfused with $NCX_{IF}$ (50 units/ml) for 5 min and the $Ca^{2+}$-entry and $Ca^{2+}$-exit reactions were monitored by performing a second abrupt-0Na in the same cardiomyocyte. ***C***. The data representing the typical effects of $NCX_{IF}$ on Ca-entry and $Ca^{2+}$-exit modes (see panel B) were normalized. The trace-a represents the control before exposure to $NCX_{IF}$, and the trace-b depicts the recordings obtained after exposure of the same cardiomyocyte to $NCX_{IF}$ (50 units/ml) for 5 min. The $Ca^{2+}$-exit rate constant ($k$) was calculated from the signal obtained by abrupt $Na^+$ removal and is presented as the percentage of the control rate constant. The control rate constant (100%) represents $k = 0.24 \pm 0.047\ s^{-1}$. ***D***. Maximal rates (first derivative) of each reaction are presented as the percentage of control. The control rate (100%) represents 157.1 ± 37.2 nM $[Ca^{2+}]_i \cdot s^{-1}$ for the $Ca^{2+}$-entry phase and 230.7 ± 54.8 nM $[Ca^{2+}]_i \cdot s^{-1}$ for the $Ca^{2+}$-exit phase. The amplitude of the $Ca^{2+}$-entry mode was measured in the presence and absence of $NCX_{IF}$ under the conditions described in panel ***B***. The control amplitude (100%) represents the

$\Delta[Ca^{2+}]_i$ value of 865.2 ± 200.9 nM measured in the absence of $NCX_{IF}$. Results are represented as the mean ± SEM. The *n* values represent the data collected from cardiomyocytes isolated from different animals.

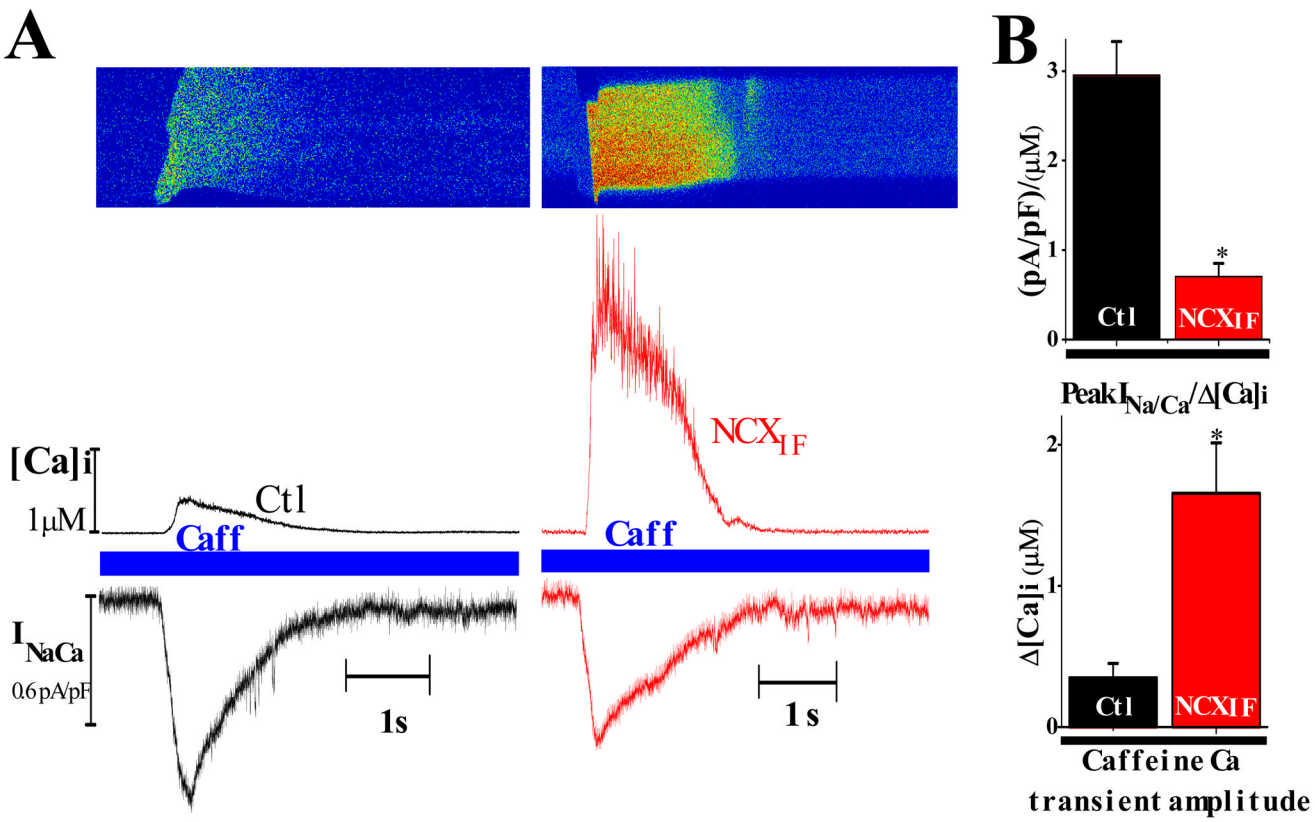


**Fig. 4. Simultaneous recordings of $I_{NCX}$ and $[Ca^{2+}]_i$ in patched cardiomyocytes after transient exposure to caffeine**

Adult rat cardiomyocytes were held at −80 mV and loaded with the $Ca^{2+}$ fluorescent dye fluo-4 through the patch pipette. $Ca^{2+}$ transients were induced by application of 5 mM caffeine (Caff) on a quiescent cell (see Materials and Methods). *A*. Typical recordings of $I_{NCX}$ and $[Ca^{2+}]_i$ from a control (left) or $NCX_{IF}$-loaded cell (right). Representative line scan image (upper panel), corresponding $[Ca^{2+}]_i$ values (middle trace), and the simultaneous recorded $I_{NCX}$ (lower trace). *B*. Upper chart, mean peak $I_{NCX}$ normalized to $\Delta[Ca^{2+}]_i$ in control (n = 10) and $NCX_{IF}$-loaded cells (n = 16, *P < 0.01). Lower chart, the mean values of Ca2+ transient amplitudes in control (n = 10) and $NCX_{IF}$-loaded cells (n = 16, *P < 0.01). The *n* represents the number of independent experiments.

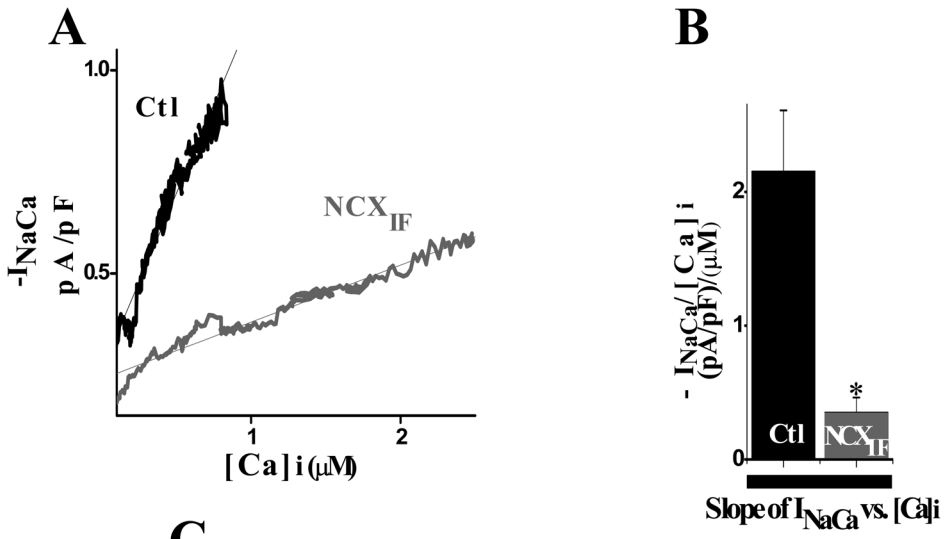


C

| *Control* | | | *$NCX_{IF}$* | | |
|---|---|---|---|---|---|
| [Ca]i range (nM) | Cells No | Exp No | [Ca]i range (nM) | Cells No | Exp No |
| 73-137 | 5 | 8 | 100- 170 | 4 | 11 |
| 141-154 | 5 | 7 | 177- 352 | 4 | 15 |
| 158-186 | 5 | 6 | 366-797 | 3 | 11 |
| 190-229 | 4 | 5 | 799-1165 | 2 | 8 |
| 234-437 | 3 | 4 | 1179-2426 | 1 | 6 |
| 438-762 | 2 | 2 | | | |

**Fig. 5. Effect of directly loading $NCX_{IF}$ into the cytoplasm on $I_{NCX}$ during $[Ca^{2+}]_i$ rise**

Cardiomyocytes were transiently exposed to 5 mM caffeine as described in Materials and Methods. The caffeine-evoked $I_{NCX}$ and $[Ca^{2+}]_i$ values were measured simultaneously and then plotted as indicated. The results represent the rising phase of the caffeine $[Ca^{2+}]_i$ transient (starting from the beginning of $[Ca^{2+}]_i$ upstroke until it peaked) ***A***. The average values of $I_{NCX}$, obtained at a given $[Ca]_i$ value, were plotted for $NCX_{IF}$-loaded or control (-$NCX_{IF}$) cardiomyocytes as indicated. ***B***. The slopes of $I_{NCX}$ vs. $[Ca^{2+}]_i$ were calculated by fitting the data for each individual experiment (n = 10 for control cells and n = 15 for $NCX_{IF}$-loaded cells, $P < 0.001$). ***C***. Different ranges of $[Ca^{2+}]_i$ values (observed in each specific experiment) were plotted *vs.* appropriate levels of $I_{NCX}$, as described in panel *A*.

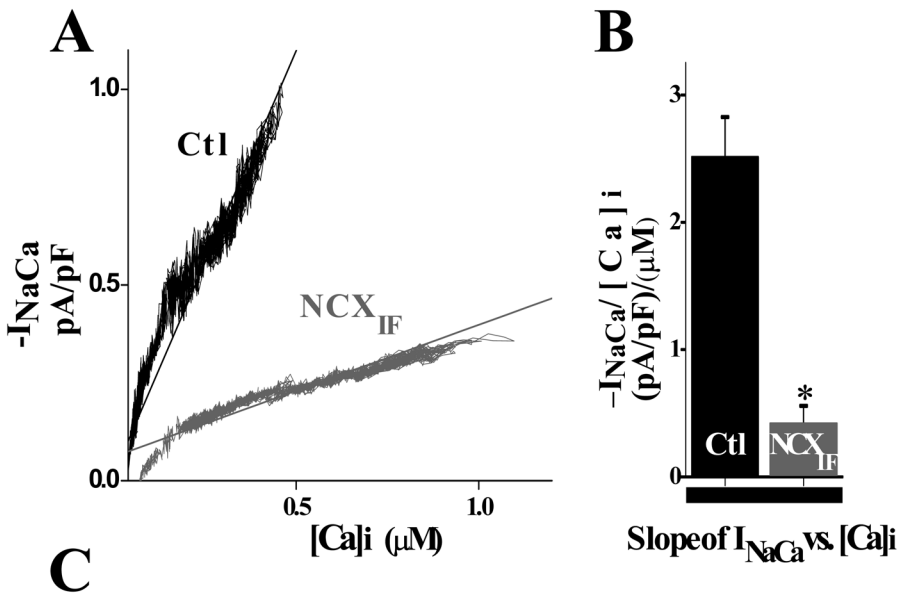


C

| *Control* | | | *$NCX_{IF}$* | | |
|---|---|---|---|---|---|
| [Ca]i range (nM) | Cells No | Exp No | [Ca]i range (nM) | Cells No | Exp No |
| 32-50 | 5 | 7 | 47-181 | 2 | 4 |
| 50-144 | 6 | 8 | 181-497 | 3 | 12 |
| 145-169 | 5 | 7 | 502-815 | 2 | 11 |
| 171-442 | 3 | 4 | | | |
| 443-786 | 2 | 2 | | | |

**Fig. 6. Effect of directly loading $NCX_{IF}$ into the cytoplasm on $I_{NCX}$ during the $[Ca^{2+}]_i$ decline**

The caffeine-evoked $I_{NCX}$ and $[Ca^{2+}]_i$ were simultaneously recorded and plotted as described in Figs. 4 and 5. The data were obtained by taking the decline phase of the caffeine-induced $Ca^{2+}$ transient (starting from the $I_{NCX}$ peak until the baseline was reached). ***A***. The average $I_{NCX}$ values (for given $[Ca^{2+}]_i$ levels) were plotted for $NCX_{IF}$-loaded or control cardiomyocytes (-$NCX_{IF}$). ***B***. The $I_{NCX}/[Ca^{2+}]_i$ curves were fitted by linear regression and the obtained slopes were averaged as indicated (n = 9 for control cells and n = 12 $NCX_{IF}$-loaded cells, $P < 0.001$). The *n* values represent the number of independent experiments. ***C***. The observed ranges of $[Ca^{2+}]_i$ values (obtained in each specific experiment) were plotted *vs.* $I_{NCX}$, as described in Fig. 5.